# Theoretical study of the heteroepitaxial growth of Pd on Cu(111), Pd on Ni(111), Ni on Pd(111), and Cu on Pd(111) using a semiempirical method

F. R. Negreiros,[1,*] E. A. Soares,[1] A. de Siervo,[2,3] R. Paniago,[1] V. E. de Carvalho,[1] and R. Landers[2,3]
[1]*Depto. de Física, ICEx, Universidade Federal de Minas Gerais, CP702 Belo Horizonte, MG, Brazil*
[2]*Instituto de Física Gleb Weteghim, Universidade Estadual de Campinas, 13083-970 Campinas, SP, Brazil*
[3]*Laboratório Nacional de Luz Síncrotron, 13084-971 Campinas, SP, Brazil*
(Received 3 November 2009; revised manuscript received 15 January 2010; published 24 February 2010)

Heteroepitaxy has been widely studied by many different theoretical and experimental techniques. Each technique focuses on some features of the growth process, and only by combining the information each provides a full characterization can be given. In this work, the growth of Pd on Ni(111), Pd on Cu(111), Cu on Pd(111), and Ni on Pd(111) is studied with a purely energetic approach which consists of determining a unit cell with a size that depends on the relation between the lateral misfit of the deposited film and the substrate. The energetic is evaluated using a semiempirical coupled with a genetic algorithm global search method to determine with accuracy the relaxation magnitudes of the system. With this approach, features such as interlayer spacings, variation in the film's lattice parameter with coverage, and diffusion influence in the growth process are studied qualitative and quantitatively. The results obtained are directly compared with experimental findings from literature and also presented in this work. The theory-experiment comparison shows that the methodology used is successful in describing qualitatively most features of all four systems. However, for the Pd on Cu(111) case, poor agreement is found, and the analysis of the influence of diffusion and temperature suggests that a somewhat complex alloy formation in the interface is expected for this particular system.

DOI: 10.1103/PhysRevB.81.085437 PACS number(s): 68.35.Gy, 68.35.Md, 68.43.−h, 31.15.bu

## I. INTRODUCTION

Surface alloys have been the focus of intense work in these last decades due mainly to their unique properties as a result of the combination of a terminated surface and the possibility of formation of stable alloy phases that happens only at the surfaces. Experimental techniques[1,2] have been widely used in the determination and characterization of the structural, electronical, and chemical properties of these systems. Reflection high-energy electron diffraction (RHEED), low-energy electron diffraction (LEED), x-ray photoelectron spectroscopy (XPS), x-ray photoelectron diffraction (XPD), ultraviolet photoemission spectroscopy (UPS), and scanning tunneling microscopy (STM) are among the most common. They provide much detailed information, such as the following: determination of the growth mode of the deposited film; characterization of the diffusion of the deposited material into the substrate as a function of the surface temperature; critical layer for the transition of pseudomorphic-incommensurate growth mode; determination of the coverage in the transition between pseudomorphic-incommensurate type of growth; determination of the interlayer spacing of the layers close to the surface and the average interlayer spacing of the whole deposited film. In the attempt to simulate these features, it is clear that the accurate qualitative and quantitative reproduction of just one of them is already a very challenging task to any theoretical method.

Many theoretical studies[1,3,4] were already performed using *ab initio* and semiempirical methods. Usually, an idealization is made in some degree, and generally they are very successful qualitatively, but accurate quantitative comparisons are more difficult. As an example of a theoretical approach, kinetic Monte Carlo (KMC) simulation[5–10] can be performed in order to give insight of the relevant mechanisms of heteroepitaxial growth process. Focusing on the kinetics of a dislocation formation, the type of growth, the interplanar spacings and lateral dislocation as a function of the value of the misfit between the interacting species can be determined using an off-lattice model together with an interaction potential (usually Lennard-Jones) between the particles. Good agreement between results from KMC simulations and molecular-beam epitaxy (MBE) experimental findings was obtained in all works. In this type of analysis, however, there is no emphasis in alloy formation, in the energetic of the system and in the modulation of the surface. In another example, an extended Huckel technique in the framework of the cluster approximation can be used in the study of the energetic and electronics of epitaxial growth.[11,12]

In order to increase the knowledge of heteroepitaxy processes, this work mainly focus in the energetic of heteroepitaxial growth. Although kinetic trap effects must be considered for a complete description of such system,[7] this work tries to show that such analysis is enough to reproduce many features mentioned earlier. A methodology based on an accurate determination of the system unit cell is implemented in order to avoid effects due to atoms at the edge, what makes possible an exact determination of the total energy of the crystal. For the evaluation of the energetic of the system, a quantum approximated method called Bozzolo-Ferrante-Smith (BFS) is used. It provides a fast and accurate way to determine the energy of formation of a multicomponent alloys[13] and also allows a simple description of the system in terms of strain and chemical effects. The BFS approach is coupled to a genetic algorithm (GA) technique in order to optimize the search for the best set of parameters that minimize the energy.

With this BFS-GA methodology, the growth of Pd deposited on Ni(111), Ni on Pd(111), Pd on Cu(111), and Cu on

 

Pd(111) is investigated. For these four systems, many detailed experimental results exist in the literature,[14–23] allowing a direct comparison of theoretical results with experimental ones. For each system, the type of growth is assumed to happen in a layer-by-layer mode, and features such as interlayer spacing, lateral displacement as a function of the number of deposited monolayers, and how diffusion affects the growth are investigated. An additional RHEED analysis of the lateral lattice variation with the number of deposited layers is performed for the particular case Pd on Ni(111), supplementing the results found in literature. The comparison between experimental results and theoretical predictions shows that a good agreement is obtained in most cases. In addition, we show how a purely energetic analysis is important to further increase the understanding of the role of each driving mechanism in epitaxy.[24]

In Sec. II, experimental results from literature for each system studied and the details and results of the RHEED experiment performed in this work are discussed. In Sec. III, the details of the implementation of both GA and BFS approaches together with the methodology used in the study of heteroepitaxial growth are given. In Sec. IV, the BFS results are shown and compared and in the last section the conclusion remarks are presented.

## II. EXPERIMENTAL RESULTS AND THE RHEED EXPERIMENT

Below, we briefly describe some experimental results found in the literature for the four systems studied in this work: Pd on Cu(111),[14,15] Cu on Pd(111),[17–19] Pd on Ni(111),[20–22] and Ni on Pd(111).[22,23] Not all results will be mentioned, only those that will have a direct consequence in our theoretical analysis.

### A. Pd on Cu(111)

A RHEED analysis performed by Paniago *et al.*[14] in the coverage ($n_l$) range between 0 and 10 ML at room temperature showed that the Pd film did not grow in a layer-by-layer mode, showing a more complex growth behavior. A perfect pseudomorphic growth was not observed even for low coverages ($n_l \approx 1$ ML), and for $n_l < 1$ ML there is already a large lateral expansion of the deposited film. The Pd film achieved its equilibrium lateral lattice parameter for $n_l > 2$ ML, and the reason for such behavior was attributed to surface alloying at low coverages that relaxes the strain in this system. There was no information regarding the dealloying for $n_l > 2$ ML. In another experiment by UPS, Pessa *et al.*[15] concluded that Pd grows pseudomorphic in a layer-by-layer mode for a coverage larger than 2 ML. Also, they found evidence for diffusion of Pd into substrate for temperatures of 550 K but no evidence at room temperature. In a recent experiment using medium energy ion scattering (MEIS). Howe *et al.*[16] found that a surface alloy with Pd occupying the first three layers was obtained for coverages bigger than 0.2 ML, with significant twinning observed specially for $n_l = 1.6$.

### B. Cu on Pd(111)

In a RHEED experiment performed at room temperature by de Siervo *et al.*,[17] the growth of Cu films occurred in a nearly layer-by-layer mode. The Cu film grows pseudomorphic for $n_l$ between 3–4 ML, and above the 4 ML coverage there is a discontinuous change in the lateral lattice parameter that assumes the equilibrium value of Cu. There is no indication of surface alloying at this temperature, but above this temperature alloying takes place although there was no determination on how it does. In a complementary work by de Siervo *et al.*[18] using combined low-energy electron diffraction and photoelectron diffraction, the authors confirm that there is alloy formation only for temperatures above 450 K. In another work, Li *et al.*[19] used a LEED technique to conclude that the growth of Cu is epitaxial but incommensurate for a number of layers bigger than 1, favoring an island formation growth instead of a layer-by-layer mode.

### C. Ni on Pd(111)

Using XPS, LEED, and XPD, Nascente *et al.*[22] studied the deposition of 3 ML of Ni on Pd(111) annealing the sample at 300 and 600 °C. It was found that, for annealing at 300 °C, the surface has islands of pure Ni and random alloy regions. The Ni islands are 3 ML thick and occupy 50–60 % of the surface, but the authors noted that the thickness of the Ni overlayer is an average of Ni islands with different thickness varying from 1 to 4 ML. The random alloy domain have high Ni concentration in the first and third layers (90%), and low (20–40 %) in the second one. At 600 °C, Ni diffuses almost completely to the bulk.

### D. Pd on Ni(111)

A nearly ideal two-dimensional growth of Pd on Ni(111) is reported by Terada *et al.*[21] at room temperature in their study by STM. Due to the existence of a moiré superstructure, with periodicity of $(12 \pm 1)$ Pd atoms for every $(13 \pm 1)$ Ni atoms, they concluded that the Pd film of 3 ML was not pseudomorphic but laterally displaced by $\approx 10\%$ (i.e., palladium atoms have approximately their equilibrium lattice parameter). Using XPS, LEED, and XPD, Nascente *et al.*[22] studied the deposition of 1.5 ML of Pd on Ni(111). At room temperature, they also reported a layer-by-layer growth with the Pd atoms completely covering the first monolayer and partially the second. The lateral lattice parameter of the Pd islands measured was +2.8% compared to the Ni bulk value. After annealing at 600 °C, 75% of the surface is covered by Pd islands with a lateral lattice parameter of +4.7% and the rest of the surface is covered by an $Pd_{20}Ni_{80}$ alloy grown pseudomorphic with the substrate.

A detailed study of the lateral lattice parameter (or surface atom spacing) evolution during the growth of Pd on Cu(111) (Ref. 14) and Cu on Pd(111) (Ref. 17) systems was previously performed by RHEED. To complement the results from literature, we have also performed a similar study for the Pd on Ni(111) system. An ultrahigh vacuum (UHV) molecular-beam epitaxy system with base pressure of $1 \times 10^{-10}$ mbar was used. The Ni(111) surface was cleaned

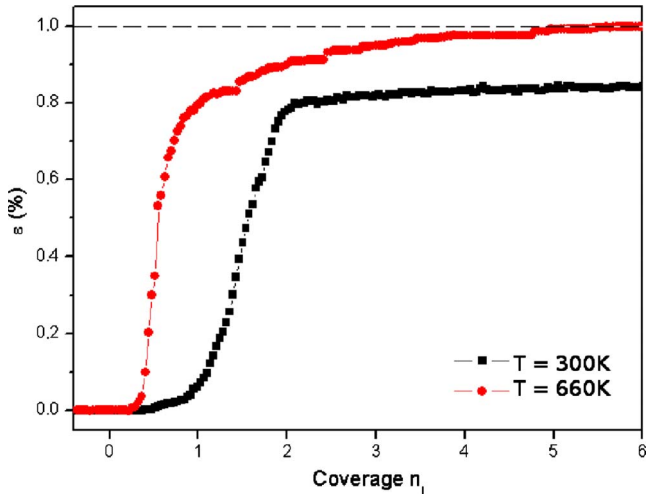


FIG. 1. (Color online) RHEED results for the lateral lattice parameter variation in Pd on Ni(111) in percentage of the Ni lattice ($\varepsilon = \frac{a - a_{\mathrm{Ni}}}{a_{\mathrm{Pd}} - a_{\mathrm{Ni}}}$) as a function of the coverage.

in UHV by cycles of argon ion sputtering with an energy of 900 eV and annealing at 970 K. Pd with 99.995% purity was evaporated from alumina crucible using an e-beam source at a 2 ML/min rate. RHEED diffraction patterns (not shown here) were recorded on a fluorescent screen using a high-sensitivity charge coupled device (CCD) camera and a video recorder linked to a computer using a software (KS400) for image processing. RHEED oscillations were observed for the first three Pd monolayers (growth at 300 K), which were used to calibrate the thickness of the film as function of evaporation time. To calculate the atom lateral spacing, which is inversely proportional to the streaks separations in the RHEED pattern, the position of the streaks were monitored as function of evaporation time (or thickness). This enables the determination of the lattice parameter with an accuracy of few tenths of a percent. The result of the lateral distance variation with coverage is shown in Fig. 1 for growth of Pd on Ni(111) at room temperature and at high temperature (600 K). At 300 K the first layer of Pd grows pseudomorphic on Ni(111), and above that ($d \geq 2$ ML) exhibits a lateral atom spacing close to that of Pd(111). The growth behavior at 600 K is quite different, the RHEED pattern evolution suggesting that the surface atom spacing is close to the value of Pd(111) even for one monolayer of Pd on Ni(111).

## III. THEORETICAL DETAILS

The theoretical study performed in this work relies on an idealization of an heteroepitaxial growth, where a Frank-Van der Merwe growth mode (layer-by-layer) is assumed, temperature effects are not fully explored, diffusion to the substrate will be studied for only small concentrations of the deposited atoms and a discontinuous change in the lateral lattice parameter in the interface between the substrate and deposited film is considered. Even with this idealized system, it will be shown that the number of atoms necessary to characterize the growth with accuracy is still large (up to an order of $10^5$ atoms), so the methodology used combine a global search method called GA with the BFS method[13,25] that quickly determines the energy of an alloy.

A surface is a large defect in a crystal; but due to its planar symmetry, its unit cell is usually composed by only a few atoms in each layer, and for this reason it can be easily treatable by most theoretical approaches. However, a lateral displacement of one or more layers is enough to completely break this symmetry, modifying the total number of atoms in the unit cell. The construction of the unit cell and its dependence on the lateral displacement are described after a brief review of the BFS method is made. Then, the BFS-GA approach is introduced, and a few considerations for the inclusion of surface alloy formation are given.

### A. BFS method

BFS is a fast and accurate method that has already been applied with a great deal of success to all the binary combinations of the Pd, Cu, and Ni elements in the (111) face. It determines the energy of formation of surface and bulk alloys with the same approach, in any configuration, i.e., allowing any type of anisotropic displacements. In BFS, the energy of formation of an alloy $\Delta H$ with $N$ atoms is given by the sum of elemental contributions $e_i$ of each atom of the alloy, i.e.,

$$\Delta H = \sum_{i=1}^{N} e_i. \tag{1}$$

The energy of the atom $i$ in the alloy is the result of a sum of two more contributions: a *strain energy* ($e_i^S$) that accounts only for structural defects and the *chemical energy* ($e_i^C$) that accounts only for defects due to the presence of atoms of different species. The strain and chemical energies are coupled by a *glue* ($g$) function, a function needed to ensure that the chemical contribution vanishes when two different atoms get farther apart. Because defects related to bond compressions are not completely described only by the strain term $e_i^S$, a relaxation term $e_i^{S2}$ needs to be included to account for anisotropic defects. Thus, the energy of formation of an alloy is written as

$$\Delta H = \sum_{i=1}^{N} (e_i^S + e_i^{S2} + g e_i^C). \tag{2}$$

In the evaluation of the strain and chemical energies, BFS makes use of the equivalent crystal theory (ECT).[26,27] The ECT is based on the universal binding-energy relation (UBER) (Ref. 28) for metals and semiconductors for the evaluation of the formation energy of a defect in a crystal. The anisotropy term used in this work is the same described by Smith *et al.*[29] and Shamus *et al.*:[30] it provides a fast way to determine the energy of formation of anisotropic compressions and is accurate for small and unilateral compressions but overestimates the gain in energy when an atom is being highly compressed in many directions at the same time. We refer the reader to Ref. 25 for a detailed description of the BFS method, its implementation, and operational equations.

A code based on the BFS methodology was written in the Surface Physics Laboratory of the Universidade Federal de Minas Gerais. To test the code, the surface segregation of noble metals in low-index faces of binary systems, among other systems, were studied and the results compared with those found in the literature that have also applied the BFS method,[25,26,29,31,32] with a perfect match between the results. All the ECT parameters and the BFS $\Delta$ parameters for Pd, Cu, and Ni were taken from Bozzolo.[25] These parameters were fitted to well-known empirical data (equilibrium lattice parameter, cohesive energy, and *bulk modulus* of each element plus the heat of solution in the dilute limit), and they have been already applied to the binary systems Pd-Ni,[32] Pd-Cu,[31] and Cu-Ni (Ref. 25) with a great deal of success.

A lateral expansion of a layer creates structural defects such as atoms on top of other atoms located in the layer below it. Considering that, for the calculation of the relaxation $e_i^{S2}$ and chemical terms in the BFS method, the information regarding the number of first and second neighbors is needed, the number of neighbors of an atom must be somehow defined. Many difficulties arise when one tries to determine with precision what is the exact interval that defines a first or second neighbor, such as an instant loss or gain of a neighbor after a short dislocation of a single atom, creating a discontinuous change in the energy. In order to avoid these type of difficulties, the following definition will be considered in this work: due to the fact that we are dealing with a (111) terminated surface, the total number of first (second) neighbors of all atoms is kept fixed in 12 (six) for bulk atoms and nine (three) for all atoms at the surface. When determining which atoms are neighbors for a bulk (surface) atom, it is considered that the 12 (nine) closest atoms are the first neighbors and the six (three) others closest ones are second neighbors. This assumption did not limit the precision of the method for two main reasons. First, the most important term regarding structural defects, especially for regions not far from equilibrium, is the strain energy, $e_i^S$, a term unrelated to any definition of number of neighbors. Second, in the definition of the chemical term, it is included a reference term that frees the total chemical energy of any structural information, meaning that the chemical energy is not affected by which definition is used.

### B. Unit cell

The systems studied in this work consist of a substrate of an element $X$ (Pd, Ni, or Cu) terminated on a (111) surface, with a film with $n_l$ layers of a different element $Y$ (also Pd, Ni, or Cu) deposited on it. For these $n_l$ layers, a lateral displacement is applied, given by the value of $\varepsilon$, in such a way that the new value of the lateral lattice parameter $a_\parallel$ is equal to $(1+\varepsilon)a_\parallel^{subs}$, considering that $a_\parallel^{subs}$ is the lateral lattice parameter of the substrate. With this definition, $\varepsilon$ represents an expansion (contraction) if it is greater (lower) than zero and its value gives the size of the displacement in percentage compared to the bulk value.

For a (111) terminated surface with no lateral expansion or contraction with a fcc symmetry, all atoms in a same layer are equivalent, and the unit cell of the system contains only one atom for each layer included in the calculation of the surface energy. Considering interactions only to second neighbors, four layers are enough to give the energy value of the (111) relaxed surface with high precision and, as a consequence, the complete unit cell consists of only four atoms. But if, for example, the topmost layer is expanded by 25%($\varepsilon$=+0.25), periodicity at the surface is achieved for a group of 16 atoms, as shown in Fig. 2. In Fig. 3, a lateral cut of the same structure of Fig. 2 is shown, where it can be seen that for each four atoms at the surface, five more atoms are needed in all substrate layers to complete the unit cell. This relation comes from the fact that the length of 100 atoms in a row at the topmost layer is the same as the length of 125 atoms at all subsurface layers. Thus, for this expansion, the unit cell consists of 16 atoms for the topmost layers and 25 for all the others. Performing this same analysis for an arbitrary value of $\varepsilon$, the number of atoms of the unit cell for any lateral expansions or contractions can be determined.

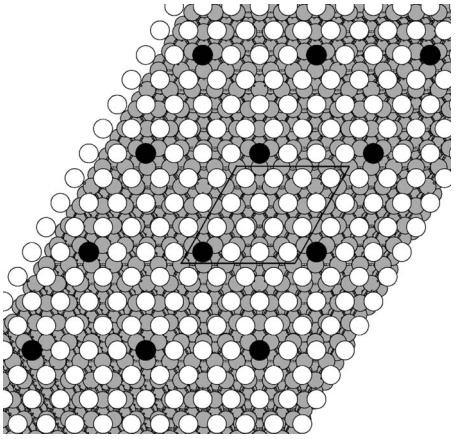

FIG. 2. This figure shows a top view of a surface terminated in a (111) facet that is subjected to a 25% lateral expansion on deposited monolayer of atoms of species $Y$ (in white) on a substrate composed of an element $X$ (atoms in gray). Atoms in black are in perfect fcc sites, and the bidimensional unit cell is highlighted.

The fact that the value of $\varepsilon$ determines the number of atoms in the unit cell is a restriction to the continuous analysis of the energy variation with $\varepsilon$: as the number of atoms increases, so does the computational time necessary to perform the energy calculation. For example, the approximated number of atoms of the unit cell of each layer equals 1 for $\varepsilon$=0, but $\approx$10 000 for $|\varepsilon|$=1,3,7,9,...%. Due to this time

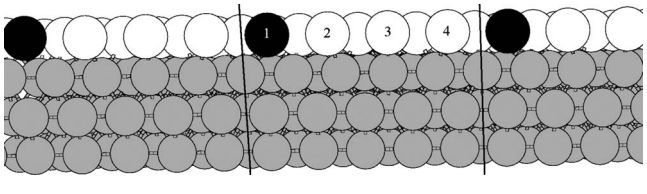


FIG. 3. A lateral cut of the crystal in the Fig. 2 is shown, where it can be seen that the unit cell consists of five atoms (in gray) for all layers of the substrate and four atoms for the deposited layers (atoms in white). This relation comes from the ratio $(1+\varepsilon)=1.25=5/4$, i.e., the periodicity changes depending on the value of the expansion.

TABLE I. For each expansion (contraction) up to $\varepsilon=5\%$ ($\varepsilon=-5\%$), this table shows the total number of atoms of the each layer of the deposited film and substrate of the unit cell.

| $\varepsilon(\%)$ | Substrate | Film |
|---|---|---|
| 0 | 1 | 1 |
| 1(−1) | 10201(9801) | 10000 |
| 2(−2) | 2601(2401) | 2500 |
| 3(−3) | 10609(9409) | 10000 |
| 4(−4) | 676(576) | 625 |
| 5(−5) | 441(361) | 400 |

issue, this work limits itself to study systems with a maximum total number of atoms of the order $10^5$, which means that $\varepsilon$, in percentage, assumes only integer values. In Table I, it is shown the number of atoms at the substrate and the deposited layers for each expansion or contraction up to 5%. The maximum value of $|\varepsilon|$ considered in this work was 15% because the maximum lattice mismatch possible for the purposes of this work happens for the Pd over Ni(111) system, with $(a_{\mathrm{Pd}}-a_{\mathrm{Ni}})/a_{\mathrm{Pd}}\approx 10.4\%$.

The amount of layers used in the evaluation of the energy is equal to $n_l+4$. To illustrate them, a lateral view of a random configuration is shown in Fig. 4. Layer S4 is a *dead* layer, representing the bulk: no atoms are moved neither their energies evaluated. Layers S3 and S2 are *passive* because their energies are evaluated but they are static. The remaining layers are *active*, i.e., their energy are calculated and they are allowed to move. The atoms in gray are of species $Y$ and all others are of species $X$. The coverage, equal to 2 ML in Fig. 4, is varied from 1 to 15 ML in this work.

When the deposited film grows pseudomorphically, due to the difference in species between film or substrate and the presence of the vacuum, a relaxation of all active atoms is necessary to optimize the energy of the surface. Thus, an accurate way to perform relaxation, including in which direction each atom has to be displaced from its original position, needs to be found. In an initial approach, allowing the same variation in the $z$ coordinate for all atoms in every layer is enough to perform this task because for the (111) surface with $\varepsilon=0$ all atoms are in perfect fcc sites and are equally distant to the atoms in the layer below. But when $\varepsilon\neq 0$, the fcc symmetry is broken and additional degrees of freedom need to be considered.

To see the effects of a lateral displacement of an entire layer in the atomic individual energy, a simple case is presented. For one layer of Pd on Ni(111) with $\varepsilon=+0.10$, the energy of each atom in the Pd layer was calculated and the results are shown in the surface plot of Fig. 5(a). In this figure, a top view of the unit cell can be seen between the two solid white lines. The two black spots pointed by small arrows in the lower part of Fig. 5(a) show the position of the atoms in perfect fcc sites, with the lowest energies. The plot shows that the expansion is responsible for the formation of two main regions: in the southwest of the unit cell the atoms are essentially on top of the atoms of the layer below, and their energy are the largest; in the northeast of the unit cell, the atoms are occupying hcp sites (pointed by a large arrow),

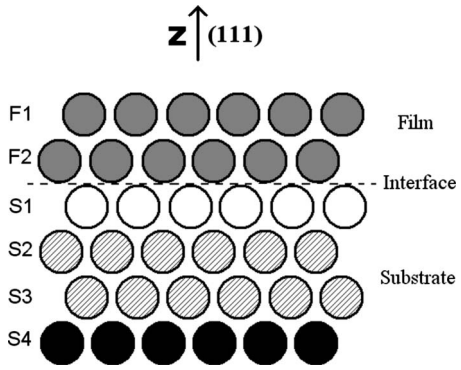


FIG. 4. For $n_l$ deposited layers of an element $Y$ on a substrate $X$ and $\varepsilon$ equals to any value, a lateral cut of the slab considered in the energy evaluation is shown. The atoms at the bottom layer, in black, are *dead*, meaning that they don't move and their energies are not evaluated. The atoms with stripes are also static, but their energies are evaluated, meaning that they are *passive*. Atoms in white and in gray are allowed to move and their energies are evaluated, so they are *active*. All atoms in gray are of species $Y$, and all others are of species $X$.

and their energies are just a little larger than the lowest-energy atoms.

Thus, in order to perform an accurate relaxation of the system, a modulation of the deposited layers is allowed before an interlayer spacing variation is performed. The modulation of an atom $i$ in any deposited layer is defined as

$$\Delta z_i = 1 - e^{A_m(r_i^{\min}-r_e)}, \tag{3}$$

where $r_i^{\min}$ is the shortest distance between the atom $i$ at layer $F(i)$ and all atoms at layer $F(i+1)$, $A_m$ is an adjustable parameter, and $r_e$ is the distance between first neighbors in the layer of the atom $i$ and the one below it, before the modulation is applied. $r_e$ is given by $\sqrt{\frac{a_X^2}{3}+\frac{a_i^2}{6}}$, where $a_i$ is the lateral lattice parameter of the layer $F(i+1)$ and is equal to $a_Y$ unless atom $i$ is located at layer $F(n_l)$ when it is equal to $a_X$. With this definition, the modulation of a layer can be compared to the energy excess due to the expansion in Fig. 5(a). In Fig. 5(b), it is shown the $\Delta z$ values for each atom in the same configuration as in Fig. 5(a), i.e., one layer of Pd deposited on Ni(111) with $\varepsilon=+0.10$ and $A_m=0.80$ Å$^{-1}$. It can be seen from Fig. 5(b) that the regions with high energy are the ones with greater values of $\Delta z$, which means that the modulation represented by Eq. (3) is quite reasonable.

The choice of an exponential repulsion in Eq. (3) deserves a few comments. First, tests with other functions (polynomials with degree ranging from 1 to 5) were made, and the exponential was, most of the time, more efficient than all others: a modulation given by Eq. (3) reduces the energy of a surface in 5% in average (when compared to a nonmodulated surface) for all systems and all expansions studied in this work, but the reduction in energy for the polynomial functions tested varied from 1% up to 6%, depending strongly on the system, the expansion and the degree of the polynomial. Second, and most important, an exponential repulsion has a more intuitive appeal: when the distance between two atoms is much smaller that the equilibrium first-

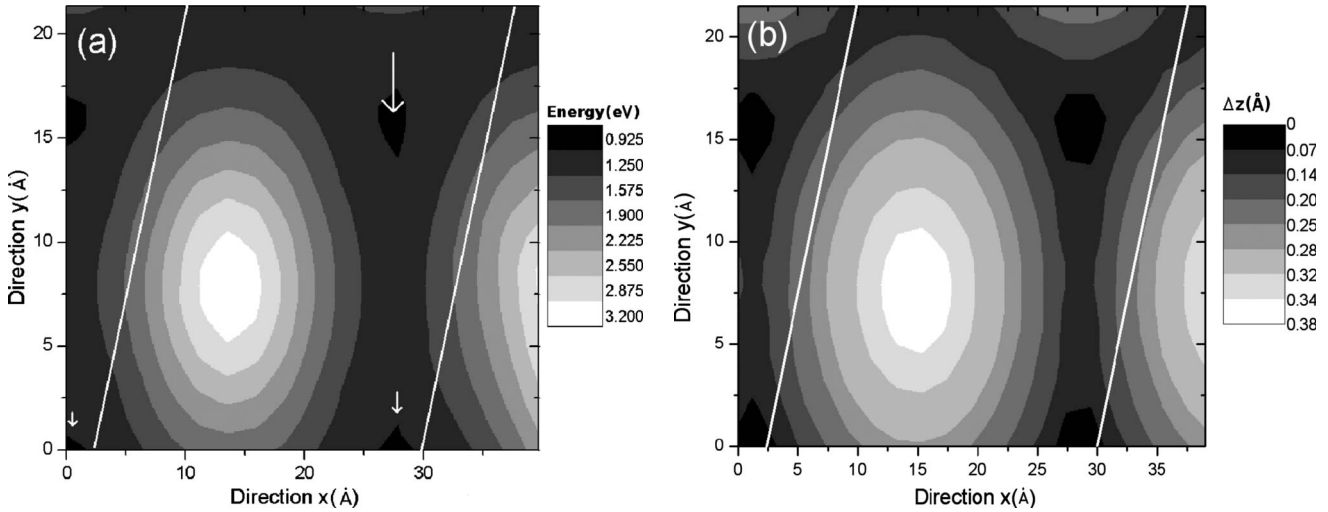


FIG. 5. Top view of the unit cell (between the two white lines) of one layer of Pd expanded laterally by 10% deposited on a Ni(111) surface. The energy of each atom of the deposited layer is shown as a function of its coordination in the xy plane. In (a), it can be seen that the expansion results in one region of high energy, where most atoms are on top of the atoms of the layer below and another region (pointed by a big arrow) where the atoms are occupying hcp sites. The two black spots pointed by a small arrow show the atoms on top of fcc sites. In (b), the same surface plot is made but with the energy replaced by $\Delta z_i$, given by Eq. (3).

neighbor distance (when an atom is on top of another, for example), it is expected by the universal binding-energy relation[28] an exponential repulsion between these two atoms. In addition, the exponential repulsion has already been used in the literature with success.[33,34] Thus, Eq. (3) was adopted and a much more complex approach (i.e., the determination of a different function for each system and each expansion) was avoided.

### C. Genetic algorithm

The GA is a global search method used to find the global minimum or maximum value of a given function. Its methodology is based on the idea of a parallel between a species evolving in a natural environment and a set of parameters of a function changing to achieve the optimum set of values, i.e., the set that gives the minimum or maximum of the function. The individual is characterized by a particular value of each parameter, and the chances of survival of an individual is represented by the value of an evaluation function that determines how close the individual is from the solution. Following the GA approach, a code was written in the Surface Physics Laboratory of the Universidade Federal de Minas Gerais using a codification with real numbers. For a more detailed description of the GA methodology used in this work, we refer the reader to Ref. 35.

For our purposes, the evaluation function is represented by the energy, which must be minimized. Each individual is characterized by the following parameters: the interlayer spacings distance equal to $d_{sub}+\Delta d_{ij}$ ($d_{sub}$ is the equilibrium distance between layers at the substrate) and the amplitude $A_m$ of the modulation given by Eq. (3). In Fig. 6, a representation of the $d_{sub}+\Delta d_{ij}$ and $A_m$ parameters are shown for the case of a pure crystal (the substrate) of an element $X$ interacting with two layers of another element $Y$ with a lateral displacement of +10%. Considering that, as a rule, the number of parameters of an individual is equal to $n_l+2$, each individual in a GA approach for the problem considered in Fig. 6 has four parameters. Each parameter is allowed to assume any value inside a specific range: for $\Delta d_{ij}$, from −30% to +30% of the value of $d_{sub}$ and for $A_m$ from 0 to 2 Å$^{-1}$. The chosen number of individuals in the population was kept fixed in 60 and only the best individual was cloned to the next generation. The mutation rate chosen was 100%, meaning that in every generation, necessarily one individual was mutated. For all cases, no more than five generations were necessary in order to find a stable population, i.e., a population with a nonchanging average energy value. For each pair of $n_l$ and $\varepsilon$, three runs starting with a population composed of different and random individuals were performed, together with a local relaxation in the $\Delta d_{ij}$ and $A_m$ parameters for the best individual obtained in each run.

The procedure described provides a fast way to find the minimum energy configuration of the system. Although there

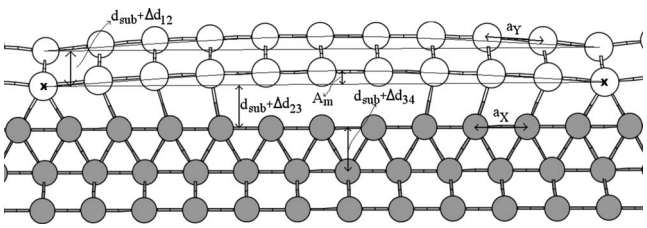


FIG. 6. Side view in the (11–2) direction of two ($n_l$=2) layers of an element $Y$ (in white) deposited on a substrate composed only of atoms of species $X$ (in gray). The following parameters are highlighted: the variation in the interlayer distance $\Delta d_{ij}$ between the first four layers, the amplitude of the modulation related to the value of $A_m$ by Eq. (3) and the lateral lattice parameters of the deposited layers ($a_Y$) and the substrate ($a_X$). The deposited layers have a lateral expansion equal to +10% ($\varepsilon$=0.10 or $a_Y$=1.10$*a_X$), and the amplitude has an exaggerated value of 2.8 Å$^{-1}$ just for illustration.

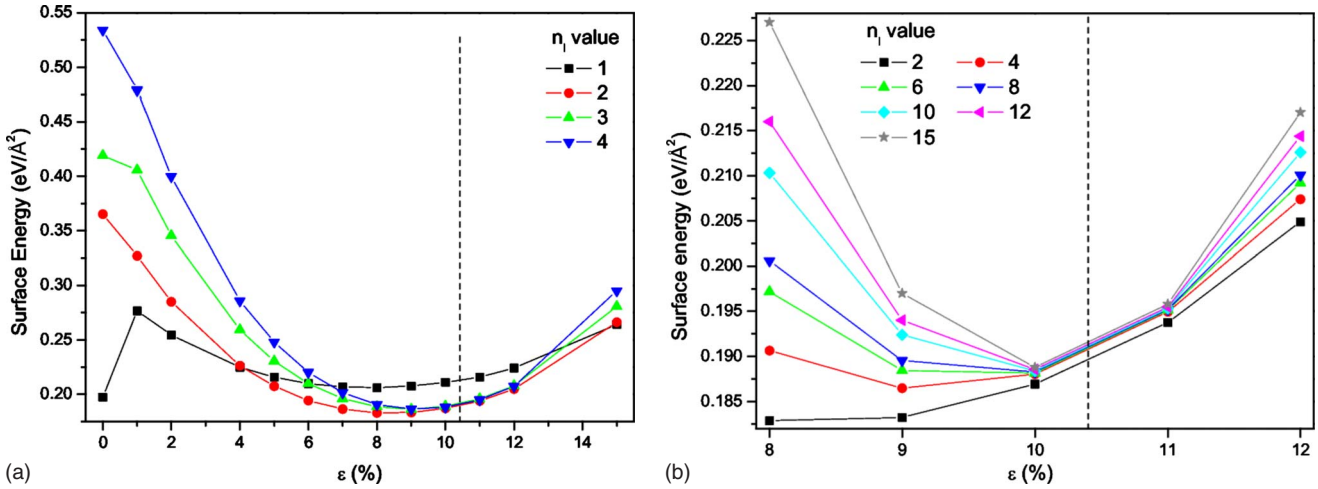


FIG. 7. (Color online) In figure (a), the surface energy of $n_l$ layers of Pd deposited on Ni(111) for $1 \leq n_l \leq 4$ is showed in function of $\varepsilon$. The dashed line represents the value of the equilibrium Pd lattice parameter, 10.4% bigger than the Ni one. In figure (b), the same type of plot is shown for a shorter interval of $\varepsilon(8\% \leq \varepsilon \leq 12\%)$ and for $n_l$=2, 4, 6, 8, 10, 12, and 15.

is no guarantee that the minimum found is the global minimum, three reasons strongly suggests so. First, the three different runs performed returned the same solution after the local relaxation was performed for almost all cases and systems. Second, the smooth behavior of the energy and interlayer spacings variation with the expansion $\varepsilon$ shows that solutions corresponding to slightly different values of the lateral displacement are almost equal. Third, for $n_l$=2 and for $\varepsilon = \pm 10\%$ (a system with just a few hundreds of atoms), grids of *energy versus* $\Delta d_{23}$ versus $A_m$ for different values of $\Delta d_{12}$ were constructed for each of the four systems studied in this work in order to confirm that the GA algorithm was exploring a large space of configurations and returning the correct global minimum.

### D. Random alloy formation

Some alloy formation in heteroepitaxy is always expected, especially at high temperatures. The amount of deposited atoms segregating to the bulk and/or forming a surface alloy depends strongly on the species involved and on the temperature, consequently changing the values of $\varepsilon$ and $\Delta d_{ij}$ described previously. A detailed analysis of all possible alloy structures for each concentration, temperature, expansion, and system is beyond the scope of this work, so a few considerations will be made in order to simplify this analysis. First, the model in Fig. 4 will remain unchanged, with all active atoms being able to exchange places with each other and with the atoms of the passive layer S2. Second, although diffusion requires a new relaxation methodology due to the break of species symmetry, no new considerations were done, considering that if the diffusion is small, local relaxations will not affect considerably the results. Third, the effects of alloying will be studied only up to two deposited monolayers: as $n_l$ increases, so does the number of parameters needed to describe the system, and satisfactory conclusions cannot be drawn. Lastly, considering the difficulty in analyzing many possible alloy structures, only random alloys are studied. The random alloys are constructed by distributing randomly the deposited atoms in 100 different ways and then evaluating the average value of the energy.

With these approximations, a number of atoms up to 50% of the total number of deposited atoms are allowed to diffuse. To which layer these atoms will segregate will depend on the system studied, and the details for each system will be given in Sec. IV. For the special case of $\varepsilon$=0, a unit cell with $\approx$100 atoms for each layer (like the one used for the $|\varepsilon|$=0.10 case) will be used. Finally, due to the absence of a global relaxation, it is important to notice that the energy of formation of the random alloys will be slightly underestimated.

## IV. RESULTS

The BFS-GA methodology explained in Sec. III was applied in the study of four systems, Pd deposited on Ni(111), Pd on Cu(111), Ni on Pd(111), and Cu on Pd(111). Most experimental results agree that the growth of Pd on Ni(111) and Cu on Pd(111) occurs in a quasi-layer-by-layer mode. Ni on Pd(111) and Pd on Cu(111) have a more complex mode of growth and it is expected that our methodology will be less accurate in the description of these two systems. Nevertheless, important information on the growth mechanism, such as the alloy formation, can still be drawn from the analysis.

### A. Pd on Ni(111)

For a coverage as big as four layers, the surface energy as a function of the expansion of the deposited film is shown in Fig. 7(a). For $n_l$=1, the lowest-energy configuration occurs when $\varepsilon$=0%, suggesting that at least initially, the growth of Pd is pseudomorphic. This same curve also shows a local minimum for $\varepsilon \approx 8\%$, suggesting that temperature may change the mode of growth. This first result is in good agreement with the RHEED results presented Fig. 1, where it is shown that Pd grows pseudomorphically at 300 K, but for 660 K the deposited layer already presents a large lateral expansion. For $n_l > 1$, the minimum at $\varepsilon$=0 no longer exists,

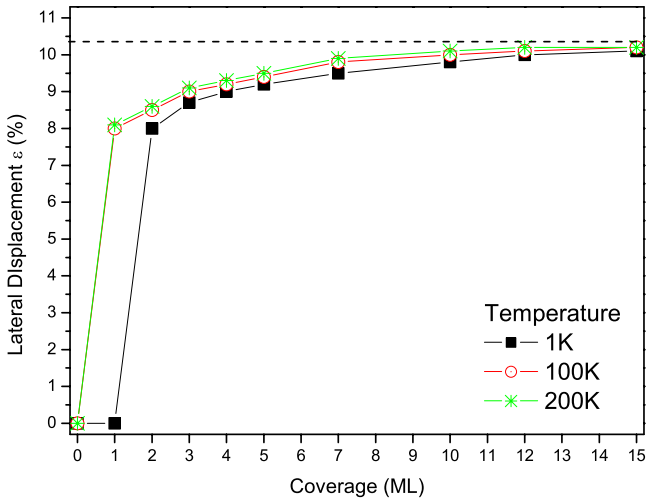


FIG. 8. (Color online) For the Pd on Ni(111) system, this plot shows the evolution of the lateral displacement ($\frac{\varepsilon a_{\mathrm{Ni}}}{a_{\mathrm{Pd}}-a_{\mathrm{Ni}}}$) as a function of the number of layers of the deposited film at 1, 100, and 200 K.

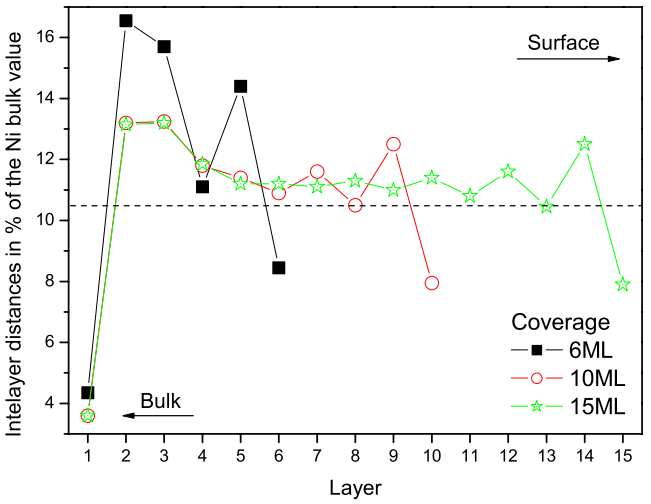


FIG. 9. (Color online) The interlayer distances $\Delta d_{i(i+1)}$ for the deposited Pd film for i ranging from 1 to $n_l$ are showed. The value of $\varepsilon$ is the one corresponding to the lowest-energy configuration for each coverage. The $x$ axis represents the $n$th layer from the interface to the surface, i.e., layer $F(n_l-x+1)$.

and the shape of the energy curve resemblance that of a wide well. As $n_l$ increases, the width of the well decreases and the global minimum gets more well defined. Also, it can be noticed that the well is asymmetric with respect to a reflection in the energy axis. The evolution of the decrease in the well's width and its asymmetric shape can be better seen in the plot from Fig. 7(b), where a shorter interval for $\varepsilon$ is shown and the number of layers varies from 2 to 15. This same figure also shows a dashed line indicating the value of the Pd-Ni misfit ($\approx$10.4%) indicating a slow progression of the lateral lattice parameter at the energy minimum toward the Pd bulk value that does achieves the misfit value only for high coverages.

In order to quantify how the lateral displacement changes with coverage and how the temperature can influence this behavior, a simple approach was created. For each specific temperature $T_c$ and coverage, the ideal lateral displacement $\varepsilon_{ideal}$ is evaluated in three steps. First, the energy of a state is reduced by a value large enough as to set the global minimum energy to zero. Second, a probability $P_i$ for each state $i$ is calculated using the Boltzmann factor, which associates the energy of a state with a normalized probability given by $P_i=e^{(-E_i/KT_c)}/\Sigma_i\, e^{(-E_i/KT_c)}$. Lastly, the value of $\varepsilon_{ideal}$ is determined summing the weighted probabilities, i.e., $\varepsilon_{ideal}=\Sigma_i\, P_i\varepsilon_i$. It should be noted that all calculated energies are in eV/Å$^2$, which means that the temperature values obtained with this three-step approach are inaccurate. Nevertheless, the motivation is the description of the qualitative change in the growth process when there is an increase in temperature, and not on the temperature value itself.

Following this approach, the equilibrium $\varepsilon_{ideal}$ values as a function of the coverage are shown in Fig. 8 for three different temperatures, 1, 100, and 200 K. A comparison with RHEED results presented earlier in Fig. 1 gives a good agreement considering the qualitative behavior of a temperature increase during the growth. In addition, the lateral lattice value as the coverage increases is well reproduced, deviating from experimental results by 10%. Nevertheless, the predicted value of the coverage when the Pd film achieves its equilibrium lattice parameter is significantly higher than the predicted experimental value, between 10 and 15 ML, depending on the temperature. It is also worth to notice that Nascente *et al.*[22] also reported a lateral expansion between +2.8% and +4.7% for a coverage of 1.5 ML, depending on the temperature, which also supports our results.

In addition to the energy minimum, our methodology also provides the interlayer spacings of the deposited film. For the lateral expansion $\varepsilon$ equal to the lowest-energy configuration taken from Fig. 7, Fig. 9 shows the values of $\Delta d_{ij}$ for all deposited Pd layers and for a few selected coverages. When the value of $\varepsilon$ lies between two integer values (for example, when $n_l$=6, $\varepsilon$=9.5%), an weighted average of the values of $\Delta d_{ij}$ for the two nearest values of $\varepsilon$ is performed. It can be seen from Fig. 9 that for a coverage of 6 ML, the values of $\Delta d_{ij}$ differ considerably from the bulk, with an overall expansion compared to the bulk values (indicated by the dashed line). The expansion of the interlayer distances is a response to the lateral contraction that exists for all coverages below 15 ML, and as expected, they get closer to the bulk value as the coverage increases. Also, it can be noticed that such layers present an oscillatory pattern near the misfit value for coverages inside the $4<n_l<15$ range.[11] For a coverage bigger than 6 ML, the distance between the first (second) and second (third) layers is equal to −2.4% (+1.1%) of the palladium interlayer distance, which is the expected interlayer spacings of a perfect infinite (111) crystal of pure Pd predicted by equivalent crystal theory.[36] Thus, for such coverages, the Pd surface is not affected by the Pd-Ni interface anymore.[37]

### *Diffusion of Pd on Ni(111)*

A BFS analysis on the diffusion of Pd on Ni(111) was already made by Bozzolo *et al.*[32] for a perfect fcc lattice with

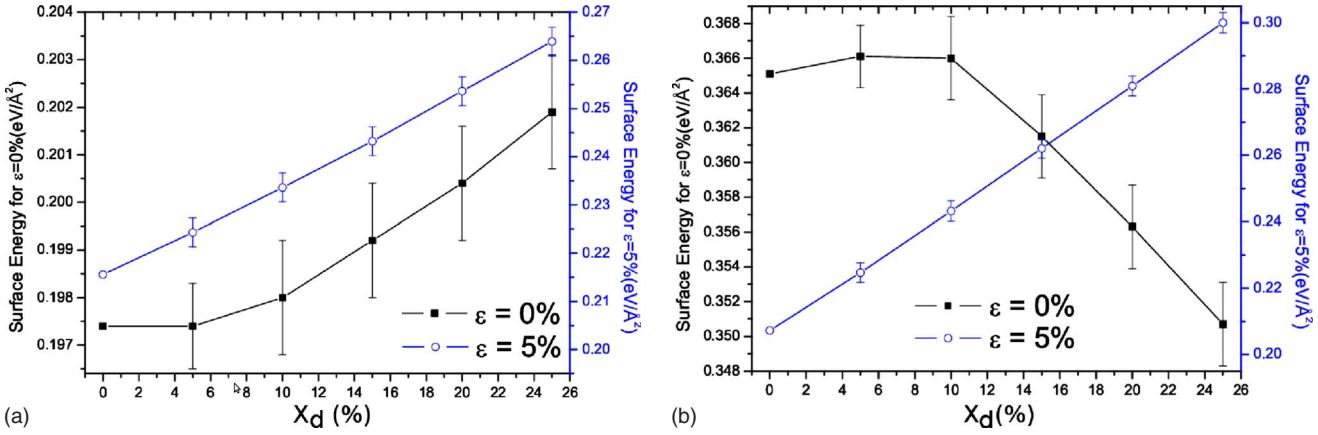


FIG. 10. (Color online) Surface energy in function of the concentration $x_d$ of Pd diffusing to the second layer below the deposited film for (a) $n_l=1$ and (b) $n_l=2$. For each plot, two values of $\varepsilon$ (0% and 5%) are analyzed. The error bar is evaluated calculating the energy difference between the lowest energetic configuration found (among the 200 tested) and the average value.

a fixed lattice parameter. For a coverage of 1.1 ML of Pd, the authors describe that the surface is filled only by Pd atoms at room temperature with the remaining atoms diffusing to the third layer. At 1000 K, a $Pd_{80}Ni_{20}$ alloy is formed at the surface with the remaining Pd atoms diffusing to the first three layers below the surface. For higher coverages, the surface layer is still mostly filled by Pd, and the Pd concentration for layers below follows an oscillatory pattern. With these results in mind, we remake the same analysis considering now the influence of a lateral displacement of the deposited film. In order to do so, for the case $n_l=1$ ($n_l=2$), the energy variation when Pd atoms in layer F1 (F2) exchange sites with Ni atoms at layer S2 was studied.

Figure 10 shows how the surface energy changes when $x_d$, the percentage of the deposited atoms that diffuses to layer S2, varies from 0 to 26%. From this figure, it can be seen for $\varepsilon=0\%$ that a small diffusion up to 10% is expected for $n_l=1$ and for $n_l=2$ diffusion is expected for much higher concentrations and can reduce the total surface energy in 5%, depending on the value of $x_d$. Repeating the same analysis for $\varepsilon=5\%$ for both coverages, we conclude that diffusion is not expected in any circumstance, only increasing significantly the total energy. For any other value of $\varepsilon$ bigger than 5%, diffusion increases even more the total energy. Considering that, for $n_l>2$, the energy of the most stable configuration is at least 50% lower than the configuration with $\varepsilon=0$, diffusion of Pd into the bulk is not expected for any coverage greater than 1 ML.

As described in Sec. II, for coverages below 1.5 ML, diffusion was predicted by Nascente *et al.*[22] only after annealing at 600 °C, what agrees well with our results. In summary, our analysis of diffusion suggested that even if there is some diffusion of Pd on the Ni surface, it should be small and the results presented earlier, i.e., Figs. 8 and 9, should not change at room temperature and for coverages above 1 ML.

### B. Cu on Pd(111)

For coverages up to 5 ML, Fig. 11 shows how the surface energy varies with $-\varepsilon$. This plot shows the presence of two well defined minima that competes as the coverage changes. Up to a coverage of 3 ML, the lowest-energy configuration occurs for a pseudomorphic growth type, at $\varepsilon=0$. For $n_l>3$, the lowest-energy configuration occurs at $\varepsilon\approx-8\%$, close to the Cu-Pd misfit value of −7.1%. In addition, the high-energy region that separates the two minima gets smaller as the coverage increases, but it exists for coverages as large as 12 ML. The shape of the well around the Cu-Pd misfit also changes with coverage, as it can be seen in Fig. 12, where the surface energy values in the interval $4\%\leq-\varepsilon\leq12\%$ for $n_l=5$, 7, 10, and 14 is shown.

The same temperature analysis done for the Pd on Ni(111) case was made for the Cu on Pd(111) system, with one additional feature. Given that there are two minimums for almost all coverages, we first determine if the growth is pseudomorphic or incommensurate, by evaluating if the probability at $\varepsilon=0$ is lower than the summed probability of all states with $4\%\leq-\varepsilon\leq12\%$ at a specific temperature $T_c$. If the growth is incommensurate, then an analysis of the value

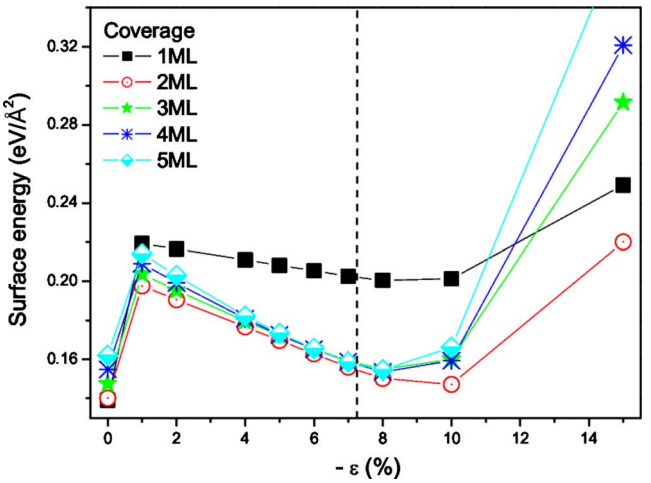


FIG. 11. (Color online) Surface energy of $n_l$ layers of Cu deposited on Pd(111) for $1\leq n_l\leq5$ is showed in function of $-\varepsilon$. The dashed line represents the value of the misfit between Cu and Pd, −7.1%.

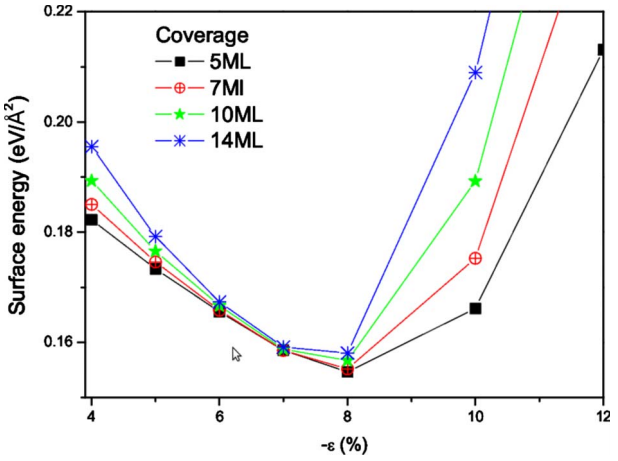


FIG. 12. (Color online) The same type of plot as in 11 is shown for a shorter interval of $\varepsilon(4\% \leq -\varepsilon \leq 12\%)$ and for $n_l=5$, 7, 10, and 14.

of $\varepsilon_{ideal}$ on this interval is made. If not, then $\varepsilon_{ideal}$ is simply set as zero. The result of such analysis is presented in Fig. 13 for three different temperatures, 1, 100, and 200 K, where it is shown that the critical coverage for the transition varies from 2 to 4 ML depending on the temperature. Compared to the 3–4 ML obtained with RHEED by de Siervo *et al.*,[17] a good agreement is found, although there are no experimental results for different temperatures to confirm the qualitative behavior obtained.

The interlayer distances for $n_l=5$, 7, 10, and 14 are shown in the plot from Fig. 14 for $\varepsilon=-7.1\%$. It can be seen that, as the coverage increases, the values are almost equal to the Cu equilibrium value (represented by a dashed line), except for the layers closer to the surface and the ones closer to the interface. It is also clear that the values of $\Delta d_{12}$, $\Delta d_{23}$, and $\Delta d_{n_l(n_l+1)}$ do not change for coverages bigger than 5 ML, suggesting that the Cu surface is not affected by the Pd-Cu interface for $n_l>5$.

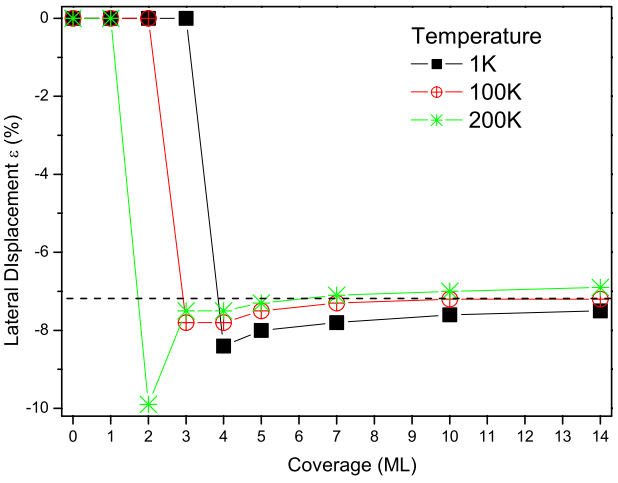


FIG. 13. (Color online) Predicted lateral displacement $\varepsilon$ in function of the number of deposited layers of Cu on Pd(111) at 0, 100, and 200 K.

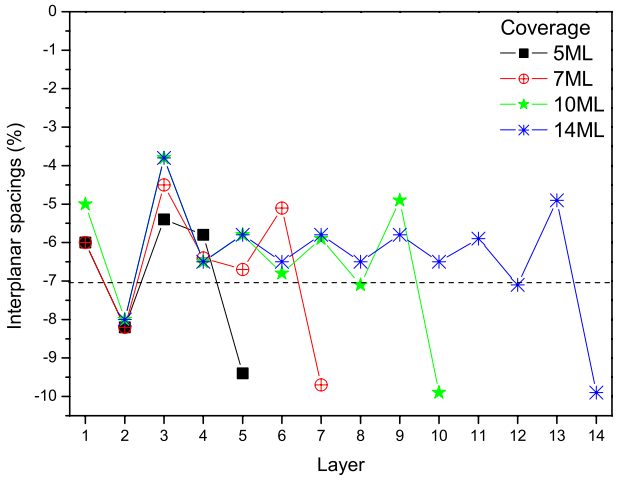


FIG. 14. (Color online) For $\varepsilon=-7.1\%$, the plot shows the $\Delta d_{i(i+1)}$ values for $i$ ranging from 1 to $n_l$ for $n_l=5$, $n_l=7$, $n_l=10$, and $n_l=14$. The $x$ axis represents the $n$th layer from the interface to the surface, i.e., layer $F(n_l-x+1)$.

### *Diffusion of Cu on Pd(111)*

As shown in the last section, it is expected that the growth of Cu on Pd up to 2 ML is pseudomorphic, even at high temperatures. Thus, the analysis of diffusion will be performed considering only the case $\varepsilon=0$. Table II shows how the energy and the interlayer spacings change when the copper atoms are allowed to diffuse to different layers toward the bulk. From the results shown in the table, it can be drawn that the most stable configurations occur for a Pd-enriched F1 layer, followed by a Cu-enriched F2 layer and mixed S1 and S2 layers. The reduction in energy is equal to 30%, what tells that the predicted value of the critical coverage for the pseudomorphic-incommensurate transition is underestimated in case alloying takes place, as expected considering that there is a Cu-Pd surface alloy instead of a Cu-Pd interface. Thus, the $T=100$ K and $T=200$ K curves shown in Fig. 13 could be incorrect if these temperature values are large enough to stimulate the diffusion of Cu on the Pd(111) surface.

In the same Table II, the interlayer spacings for each distribution are also shown. Although there are few qualitative changes due to alloying, the size of the contraction of the first three layers are very sensitive to the atomic distribution, with variations of up to (5%) (0.12 Å) for each layer. Thus, the interlayer distances presented in Fig. 14 will all suffer a considerable change (as large as 50%) in magnitude if a surface Cu-Pd alloy is formed and such changes could serve as an indication of the formation of Cu-Pd alloys during an experiment.

### C. Ni on Pd(111)

Repeating again the same analysis performed for the Cu-Pd system (see supplementary material), the plot in Fig. 15 was drawn. The lateral displacement is shown as a function of the coverage for the three temperature values, 1, 100, and 200 K. It can be seen that the change pseudomorphic-incommensurate occurs at 2 ML for all temperatures and that

TABLE II. For a coverage of 2 ML and $\varepsilon=0$, the table shows the energy and the interlayer spacings as a function of percentage of deposited copper atoms that diffuse to the bulk ($x_d$). $x_{Cu}(L)$ is the composition of copper (in percentage) at the layer $L$.

| $x_d$ | $x_{Cu}$(F1) | $x_{Cu}$(F2) | $x_{Cu}$(S1) | $x_{Cu}$(S2) | Energy (eV/Å$^2$) | $(\Delta d_{34};\Delta d_{23};\Delta d_{12})$ |
|---|---|---|---|---|---|---|
| 0 | 100 | 100 | 0 | 0 | 0.14018 | (1.1;−2.9;−15.1) |
| 20 | 60 | 100 | 40 | 0 | 0.13163 | (−0.3;−5.6;−11.0) |
| | 60 | 100 | 0 | 40 | 0.11063 | (−0.9;−2.8;−11.2) |
| | 100 | 60 | 40 | 0 | 0.14027 | (−1.1;−3.2;−10.4) |
| | 100 | 60 | 0 | 40 | 0.12589 | (−1.3;−1.0;−10.0) |
| | 80 | 80 | 40 | 0 | 0.13435 | (−0.6;−4.0;−10.6) |
| | 80 | 80 | 0 | 40 | 0.11707 | (−1.0;−1.6;−10.8) |
| | 80 | 80 | 20 | 20 | 0.12097 | (−1.0;−2.8;−10.8) |
| 40 | 20 | 100 | 0 | 80 | 0.10189 | (−5.2;−6.2;−7.4) |
| | 20 | 100 | 40 | 40 | 0.09939 | (−2.6;−6.4;−7.4) |
| | 60 | 60 | 80 | 0 | 0.12275 | (−2.2;−6.4;−6.2) |
| | 60 | 60 | 0 | 80 | 0.10877 | (−3.0;−1.2;−6.6) |
| | 60 | 60 | 40 | 40 | 0.10622 | (−2.8;−3.2;−6.4) |

a contraction of 1–2 % on the Ni deposited film is predicted for coverages smaller than 4 ML. Unfortunately, there are no experimental results studying the lateral displacement, so direct theory-experiment comparison is not possible. The analysis for the interlayer distances shows a similar behavior between the Ni on Pd(111) and Cu on Pd(111) systems.

### *Alloying*

Given that for 2 ML, the growth has a higher chance of being incommensurate than pseudomorphic, the analysis of diffusion will be performed considering both cases, $\varepsilon=0$ and $\varepsilon=-10\%$. For $\varepsilon=0$, Table III shows how the energy and the interlayer spacings change when the Ni atoms are allowed to diffuse to different layers toward the bulk. As it occurred for the Cu-Pd system, the most stable configurations occur for a Pd-enriched F1 layer, followed by a Ni-enriched F2 layer and mixed S1 and S2 layers. The reduction in energy is equal to 20%, suggesting that the predicted value of the critical coverage for the pseudomorphic-incommensurate transition is underestimated in case alloying takes place. But due to the small energy decrease due to alloying and the much lower energy of the $\varepsilon\approx-10\%$ case, it is expected that the effect of diffusion is much less pronounced compared to the Cu-Pd case. For the $\varepsilon=-10\%$ case, this same analysis gives that diffusion always increases the energy, no matter what composition or distribution is given. For $x_d=20\%$, the most stable configuration has an energy of 0.23318 eV/Å$^2$, 30% higher compared to the $x_d=0\%$ case, so in the end diffusion is energetically unfavorable if the deposited Ni film has an incommensurate type of growth. Therefore, the analysis of diffusion for both $\varepsilon\approx0$ and $\varepsilon\approx-10\%$ cases tells that the results presented in Fig. 15 are still valid for high coverages and also that the critical coverage of 2 ML is underestimated for temperatures bigger than 1 K.

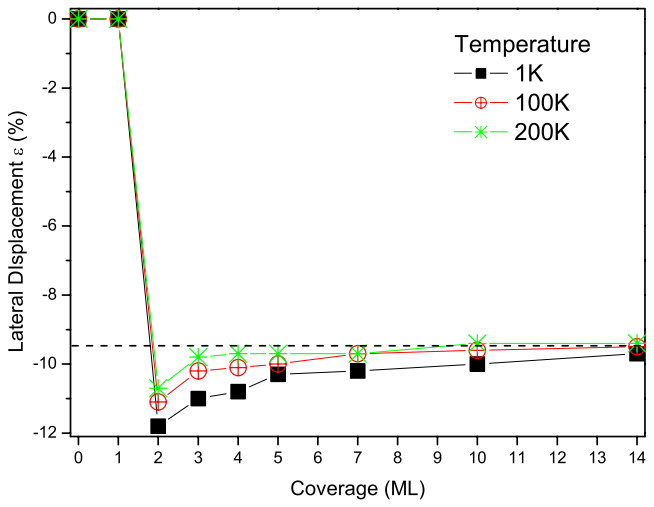


FIG. 15. (Color online) Evolution of the equilibrium value of $\varepsilon$ in function of the number of deposited layers of Ni on Pd(111) at 1, 100, and 200 K.

As a final comment on the growth of Ni on Pd(111), the composition of the surface layers obtained by Nascente *et al.*[22] (first and third layers rich in Ni and a second one poor in Ni) is quite different from the lowest-energy configuration predicted by our methodology shown on Table III. This difference could be related, among other reasons, to the influence of temperature in the diffusion process.

### D. Pd on Cu(111)

Repeating again the same analysis performed for the Pd-Ni system (see supplementary material), the plot in Fig. 16 was drawn. A similar behavior compared the Pd on Ni(111) case shown in Fig. 8 is obtained, which is not a surprise since one of the greatest differences between these two systems in the BFS methodology is the chemical $\Delta$ parameter, that has little influence in these specific results since

TABLE III. For a coverage of 2 ML and $\varepsilon=0$, the table shows the energy and the interlayer spacings as a function of percentage of deposited Ni atoms that diffuse to the bulk ($x_d$). $x_{Ni}(L)$ is the composition of copper (in percentage) at the layer $L$.

| $x_d$ | $x_{Ni}$(F1) | $x_{Ni}$(F2) | $x_{Ni}$(S1) | $x_{Ni}$(S2) | Energy (eV/Å$^2$) | $(\Delta d_{34};\Delta d_{23};\Delta d_{12})$ |
|---|---|---|---|---|---|---|
| 0 | 100 | 100 | 0 | 0 | 0.20712 | (1.5;−4.3;−19.2) |
| 20 | 60 | 100 | 40 | 0 | 0.20098 | (−0.7;−8.3;−13.6) |
| | 60 | 100 | 0 | 40 | 0.18754 | (−1.3;−4.3;−13.8) |
| | 100 | 60 | 40 | 0 | 0.22885 | (−1.1;−3.9;−12.4) |
| | 100 | 60 | 0 | 40 | 0.21808 | (−1.7;−1.5;−12.6) |
| | 80 | 80 | 40 | 0 | 0.21434 | (−1.1;−5.9;−13.0) |
| | 80 | 80 | 0 | 40 | 0.20191 | (−1.5;−2.9;−13.2) |
| | 80 | 80 | 20 | 20 | 0.20493 | (−1.3;−4.1;−13.0) |
| 40 | 20 | 100 | 0 | 80 | 0.16984 | (−3.3;−4.3;−8.8) |
| | 20 | 100 | 40 | 40 | 0.16775 | (−2.9;−8.5;−8.6) |
| | 60 | 60 | 80 | 0 | 0.20163 | (−2.9;−8.3;−7.4) |
| | 60 | 60 | 0 | 80 | 0.19526 | (−3.7;−1.7;−7.8) |
| | 60 | 60 | 40 | 40 | 0.19107 | (−3.5;−4.3;−7.6) |

no diffusion was allowed. Comparing the result obtained so far with the RHEED one from literature (Paniago *et al.*[14]), no agreement is found. This difference can be related to many factors, such as a more complex growth process with the formation of islands, alloys and/or dislocations for this particular system or a larger role played by diffusion, as predicted in the literature.[16] This is investigated next.

### *Alloying*

According to the experimental results presented on Sec. II, diffusion of Pd is expected for coverages below 1 ML and for temperatures around 500 K. Earlier BFS calculations[31] on the Pd-Cu(111) alloy formation concluded that it is energetically favorable that Pd diffuse to bulk layers. For this reason, the surface energy for $n_l=1$ was evaluated as a function of the percentage of the deposited Pd atoms that diffuse to layer S2. Figure 17(a) shows the results of this analysis for $0<x_d<60$ and two different values of $\varepsilon$, 0 and 4%. From this plot, it can be concluded for $\varepsilon=0\%$ that the lowest energetic configuration occurs for a distribution of Pd atoms equal to $Pd_{60}Cu_{40}$ at layer F1, $Pd_0Cu_{100}$ at S1, and $Pd_{40}Cu_{60}$ at S2. For $\varepsilon=4\%$, diffusion of Pd is still energetically favorable, but the reduction in energy is about only 0.003 eV/Å$^2$ at $x_d=10\%$. Thus, considering that the energy difference between the global minimum at $\varepsilon=0$ and the local minimum at $\varepsilon\approx5.5\%$ is almost 0.1 eV/Å$^2$, the configuration of minimum energy for $n_l=1$ occurs and for $\approx40\%$ of Pd atoms diffusing to the second layer of the Cu bulk, with the remaining Pd at the surface film forming a $Pd_{60}Cu_{40}$ alloy grown pseudomorphic with the substrate.

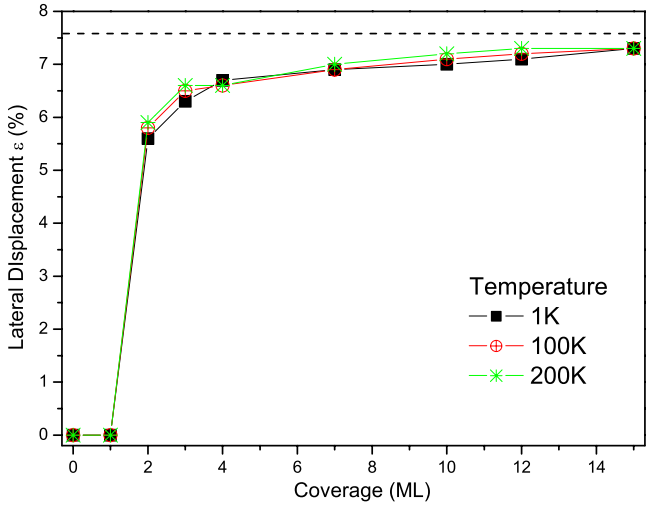


FIG. 16. (Color online) Evolution of the equilibrium value of $\varepsilon$ in function of the number of layers of the deposited film at 1, 100, and 200 K.

For $n_l=2$, considering again the BFS calculations from literature,[31] the lowest energetic configuration occurs for a F1 and S2 layers rich in Pd atom and a Cu-rich F2 layer, i.e., the Pd atoms migrate from layer F2 to layer S2. With these results in mind, the energy variation in function of $x_d$ was evaluated for five different lateral displacements and the plot shown in Fig. 17(b) was drawn. From this plot it can be concluded that diffusion greatly decreases the energy of the pseudomorphic growth, to the point that the energy of this configuration gets equal (for $x_d\approx35\%$) to the energy of the configuration with a lateral displacement of $\approx5.5\%$. So as it happens for the $n_l=1$ case, two energy minimums exist for different values of $\varepsilon$, 0 and 5.5%. For other displacements up to 6%, diffusion still reduce the energy, which means that even when the growth is incommensurate, the Pd diffusion to the bulk is still energetically favorable. Given that the two energy minimums have comparable values, there are two competing regimes for such coverage: an alloy grown pseudomorphically with a oscillatory composition of rich-Pd and rich-Cu layers and an almost perfect Pd bilayer grown incommensurate on top of a Cu(111) surface. Thus, the determination of $\varepsilon_{ideal}$ as a function of the coverage for Pd on

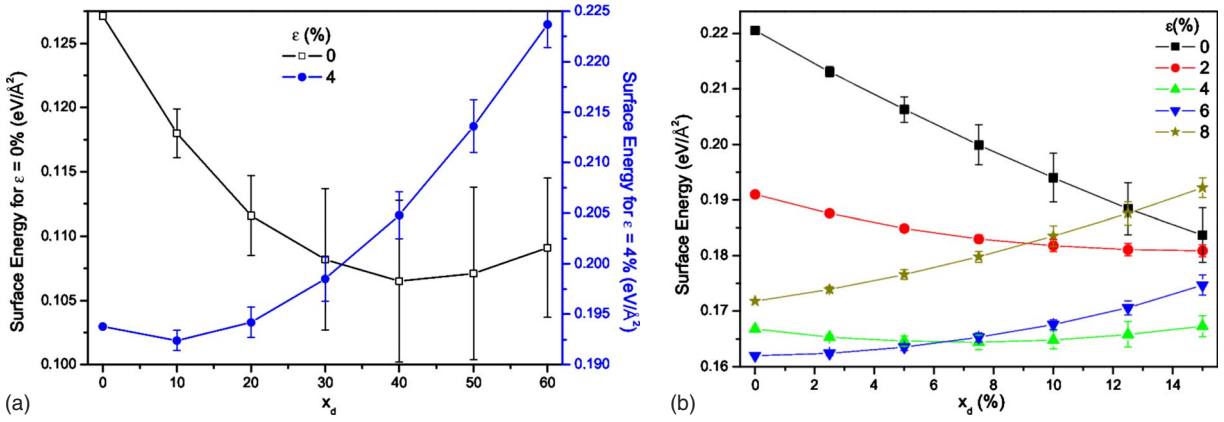


FIG. 17. (Color online) In (a), the surface energy variation as a function the concentration of Pd atoms diffusing to layer S2 in the Cu(111) substrate is shown for $n_l=1$. The leftside (rightside) $y$ axis shows the energy of the $\varepsilon=0(\varepsilon=4\%)$ case. In (b), the same plot is shown for $n_l=2$ and many different values of $\varepsilon$.

Cu(111) should somehow include at the same time the temperature and diffusion features, and the result shown in Fig. 16 oversimplified the growth process. Still, the theory-experiment differences are noteworthy and should be investigated by other methods-methodologies.

## V. CONCLUSIONS

The growth of Pd on Ni(111), Pd on Cu(111), Ni on Pd(111), and Cu on Pd(111) was studied with a purely energetic analysis. In order to accurately determine the surface energy, an approach that consisted in creating an unit cell with a changing size depending on the lateral expansion of the deposited film was adopted. The BFS method used in the calculation the energy of formation of all different configurations was coupled with a GA algorithm to determine the minimum energy and the optimum values of the interlayer spacings of the deposited film.

The results obtained for the growth of Pd on Ni(111) show that for a coverage of 1 ML, the most stable mode of growth is the pseudomorphic, but a metastable configuration exist for a lateral expansion of $\approx 8\%$, what is in good agreement with the experimental results performed also in this work and the ones from literature. For higher coverages, only one minimum energy configuration exist, with a lateral expansion slowly changing toward the Pd bulk lateral distance, which is also in agreement with experimental results. In the determination of the influence of temperature in the results obtained, the qualitative behavior was correctly reproduced: as temperature increases, the transition pseudomorphic-incommensurate mode of growth occurs in the earlier stages of growth, i.e., for lower coverages. The study of diffusion suggests that although the segregation of Pd into Ni bulk layers can reduce the energy for small lateral expansions at a coverage of 2 ML, the reduction is small and should not affect the results previously shown.

In the deposition of Cu on Pd(111), the pseudomorphic-incommensurate transition does not occur smoothly, instead it suffers a sudden change at a critical coverage. The critical coverage value depends on the temperature, between 2 ML (at 200 K) and 4 ML (at 1 K) if diffusion is not taken into account. This is in good agreement with the experimental result from literature that predicts about 4 ML at room temperature. The study of diffusion for low coverages and for a pseudomorphic epitaxy showed that this determined critical coverage is underestimated and should be at least 2 ML bigger for higher temperatures. The atomic distribution for the lowest-energy configurations consisted in a Pd enriched first layer followed by $n_l-1$ consecutive layers with an almost 50–50 % Pd-Cu alloy.

For the Ni on Pd(111) system, as it occurred for the Cu on Pd system, there is a critical coverage when the growth is incommensurate, equal 2 ML at all temperatures. If diffusion is taken into account, a small increase of 1–2 ML in the expected critical coverage should occur, depending on the temperature. The calculated composition in each layer that minimizes the energy are: Pd-rich first layer followed by a Ni-rich second layer and Pd-Ni alloy in the consecutive layers. This distribution is quite different from the one obtained by Nascente *et al.*,[22] what suggests that temperature effects probably plays a very important role in the diffusion process.

Finally, for the growth of Pd on Cu(111), poor match between the predictions of this work and the RHEED results from literature was obtained in the analysis of the lateral expansion as a function of the coverage. However, our study of diffusion shows that the growth is much more complex compared to the other systems studied due mainly to surface alloy formation as confirmed by MEIS measurements from the literature.[16] Up to a coverage of 2 ML, two different configurations are very close in energy, each with its own atomic distribution, lateral displacement, and interlayer spacing distances. Although this does not explain the differences obtained, it shows that an analysis taking into account at least diffusion and temperature at the same time is necessary for a more accurate description of this system.

## ACKNOWLEDGMENTS

We would like to thank the Brazilian agencies CNPq and FAPEMIG for financial support. Also, we would like to thank G. Bozzolo for fruitful discussions and for providing valuable material.

*fabionr@fisica.ufmg.br

[1] D. P. Woodruff, *Surface Alloys and Alloy Surfaces (The Chemical Physics of Solid Surfaces)*, 10th ed. (Elsevier Science, New York, 2002).
[2] J. A. Rodriguez, Surf. Sci. Rep. **24**, 223 (1996).
[3] T. Dieing and B. F. Usher, Phys. Rev. B **67**, 054108 (2003).
[4] H. Dreyssé and C. Demangeat, Surf. Sci. Rep. **28**, 65 (1997).
[5] F. Much, M. Ahr, M. Biehl, and W. Kinzel, Comput. Phys. Commun. **147**, 226 (2002).
[6] T. Volkmann, F. Much, M. Biehl, and M. Kotrla, Surf. Sci. **586**, 157 (2005).
[7] M. Walther, M. Biehl, and W. Kinzel, Phys. Status Solidi C **4**, 3210 (2007).
[8] D. A. Faux, G. Gaynor, C. L. Carson, C. K. Hall, and J. Bernholc, Phys. Rev. B **42**, 2914 (1990).
[9] W. M. Plotz, K. Hingerl, and H. Sitter, Phys. Rev. B **45**, 12122 (1992).
[10] J. Kew, M. R. Wilby, and D. D. Vvdensky, J. Cryst. Growth **127**, 508 (1993).
[11] P. Hermann, D. Simon, and B. Bigot, Surf. Sci. **350**, 301 (1996).
[12] N. J. Castellani and P. Légaré, J. Phys. Chem. **98**, 9606 (1994).
[13] G. Bozzolo and J. Ferrante, Phys. Rev. B **45**, 12191 (1992).
[14] R. Paniago, A. de Siervo, E. A. Soares, H.-D. Pfannes, and R. Landers, Surf. Sci. **560**, 27 (2004).
[15] M. Pessa and O. Jylhä, Solid State Commun. **46**, 419 (1983).
[16] C. J. Howe, M. D. Cropper, T. P. Fleming, R. M. Wardle, P. Bailey, and T. C. Q. Noakes, Surf. Sci. **604**, 201 (2010).
[17] A. de Siervo, R. Paniago, E. A. Soares, H.-D. Pfannes, R. Landers, and G. G. Kleiman, Surf. Sci. **575**, 217 (2005).
[18] A. de Siervo, E. A. Soares, R. Landers, and G. G. Kleiman, Phys. Rev. B **71**, 115417 (2005).
[19] H. Li, D. Tian, F. Jona, and P. M. Marcus, Solid State Commun. **77**, 651 (1991).
[20] M. F. Carazzolle, S. S. Maluf, A. de Siervo, P. A. P. Nascente, R. Landers, and G. G. Kleiman, Surf. Sci. **600**, 2268 (2006).
[21] S. Terada, T. Yokoyama, N. Saito, Y. Okamoto, and T. Ohta, Surf. Sci. **433-435**, 657 (1999).
[22] P. A. P. Nascente, M. F. Carazzolle, A. de Siervo, S. S. Maluf, R. Landers, and G. G. Kleiman, J. Mol. Catal. A: Chem. **281**, 3 (2008).
[23] M. F. Carazzole, S. S. Maluf, A. de Siervo, P. A. P. Nascente, R. Landers, and G. G. Kleiman, J. Electron Spectrosc. Relat. Phenom. **156-158**, 405 (2007).
[24] M. Ohring, *The Materials Science of Thin Films* (Academic Press, New York, 1992).
[25] G. Bozzolo, in *The Chemical Physics of Solid Surfaces*, edited by D. P. Woodruff (Elsevier, New York, 2001), Vol. 10.
[26] J. R. Smith, T. Perry, A. Banerjea, J. Ferrante, and G. Bozzolo, Phys. Rev. B **44**, 6444 (1991).
[27] A. M. Rodríguez, G. Bozzolo, and J. Ferrante, Surf. Sci. **289**, 100 (1993).
[28] J. H. Rose, J. R. Smith, and J. Ferrante, Phys. Rev. B **28**, 1835 (1983).
[29] J. R. Smith and A. Banerjea, Phys. Rev. B **37**, 10411 (1988).
[30] S. Funk, G. Bozzolo, J. E. Garcés, and U. Burghaus, Surf. Sci. **600**, 195 (2006).
[31] A. Canzian, H. Mosca, and G. Bozzolo, Surf. Sci. **551**, 9 (2004).
[32] G. Bozzolo, R. D. Noebe, J. Khalil, and J. Morse, Appl. Surf. Sci. **219**, 149 (2003).
[33] A. Tkatchenko, Phys. Rev. B **75**, 085420 (2007).
[34] A. Tkatchenko, N. Batina, and M. Galván, Phys. Rev. Lett. **97**, 036102 (2006).
[35] M. L. Viana, R. Díez Muiño, E. A. Soares, M. A. Van Hove, and V. E. de Carvalho, J. Phys.: Condens. Matter **19**, 446002 (2007).
[36] F. R. Negreiros, E. A. Soares, and V. E. de Carvalho, Phys. Rev. B **76**, 205429 (2007).
[37] G. Bozzolo, J. E. Garcés, R. D. Noebe, P. Abel, and H. O. Mosca, Prog. Surf. Sci. **73**, 79 (2003).